Engineering and Technology Journal e-ISSN: 2456-3358

Volume 11 Issue 06 June-2026, Page No.- 10734-10747

DOI: 10.47191/etj/v11i06.48, I.F. – 8.595

Sustainable Thermal Performance Enhancement of a Rotating Shell-And-Tube Latent Heat Thermal Energy Storage Unit: Experimental and Numerical Investigations

Abdulrazzaq M. Saleh Aljumaily[1], Ahmed Qays Abdullah[2]

[1,2]Department of Mechanical Engineering, College of Engineering, Al-Sharqat University, Al-Sharqat, Salahaddin, 44001, Iraq

https://orcid.org/0000-0003-1263-1216[1]

ABSTRACT: Latent The use of latent heat thermal energy storage units for efficient energy recovery has been established widely, but its efficiency is still restricted by low thermal conductivity of phase change materials. In this work, an experimental and numerical investigation on the solidification process of paraffin wax in a horizontal shell-and-tube latent heat storage unit with stationary and rotating operation modes was performed. The evolution of the temperature field was measured in three different axial directions and three circumferential positions (0°, 45°, and 90°) in the case of both stationary and rotating operations with a flow rate of 2 L/min. At the same time, a three-dimensional numerical model of the solidification process was developed in ANSYS Fluent based on the enthalpy-porosity approach, and the Boussinesq approximation was used. It was found that the solidification process occurred radially from the inner pipe towards the shell, and the bottom part solidified faster than other areas due to thermal stratification. Rotational movement accelerated the solidification process, enhanced the temperature uniformity, and decreased the thermal resistance in the PCM layer. In the case of a flow rate of 2 L/min, the maximum heat gain was equal to 1117.8 kJ, and the total amount of energy .These numerical results agreed well with the experimental and benchmark results, which verified the reliability of the proposed model. These results clearly show that rotational movement is a successful enhancement method that can enhance the discharge process in the latent heat thermal energy storage system. Overall, this research shows that rotational movement is indeed a valid enhancement technique in the latent heat thermal energy storage system especially in terms of achieving faster discharge and thermal uniformity.

KEYWORDS: Latent Heat Thermal Energy Storage System; Phase Change Material; Rotational Motion; Solidification Enhancement; Thermal Energy Recovery; Shell-and-Tube Heat Exchanger.

I. INTRODUCTION

Latent heat energy storage (LHES) has received significant attention from researchers due to its effectiveness as a solution for energy management improvement in renewable energy technologies. Various researchers have studied the thermal properties of shell-and-tube latent heat storage units and found that the initial stage of the melting process is controlled by the heat conduction mechanism whereas natural convection plays a key role once the liquid phase is formed in the phase change material (PCM) region [1-6].

Fath [1] has performed an experimental study of shell-and-tube latent heat thermal storage units and found that natural convection current generated in the molten PCM plays a major role in the melting process. Likewise, Lacroix [2,3] has performed numerical analysis of shell-and-tube latent heat storage units and found that thermal stratification plays an important role in the melting and energy storage process. Hosseini et al. [4] have performed combined experimental and numerical investigation of the thermal properties of PCM storage units and established the significance of natural convection in the charging process. In addition to these works, Avci and Yazici [5] and Kibria et al. [6] illustrated that the performance of storage systems depends on geometry and operational condition. To increase the heat transfer in LHESs, several researchers suggested the application of fins, eccentrically placed tubes, multi-tube heat exchangers, and triplex heat exchanger designs. Fin surface has been proved to be an efficient way to increase the melting rate because of increased heat transfer area, as shown by Sasaguchi et al. [7]. It has been revealed by Dutta et al. [8] and Darzi et al. [9] that the heat transfer is improved due to higher buoyancy-induced flows resulting from the eccentric placement of the HTF tube. Agyenim et al. [10,11] showed that a multi-tube design reduces the melting period and increases the uniformity of the temperature distribution within the PCM phase-change region. Moreover, Esapour et al. [12] concluded that a multi-tube design has a significant effect on increasing the charging rate. Further studies on triplex heat exchangers and fins have been conducted and significant improvements in thermal performance and energy storage efficiency have been observed [13,14].

The other kind of improvement techniques includes enhancing HTF flow characteristics. Gong and Mujumdar [15] compared different charging and discharging flow arrangements and found that using the same side to feed the HTF during the two processes gives better thermal performance. The study of internal fins attached to HTF tubes by Tao et al. [16] showed that better heat transfer rates can be obtained. Also, pulsating HTF flow was found to reduce PCM melting time and improve storage effectiveness by Elbahjaoui and El Qarnia [17].

Rotational motion has become the latest promising improvement technique in the area of heat transfer and temperature distribution in latent heat storage systems. The idea of a rotating cylinder filled with PCM was suggested by Herrick and Zarnoch [18] and it was found out that the rotational motion leads to better mixing of the molten PCM and consequently to improved heat transfer. Kurnia and Sasmito [19] performed a numerical study of rotating shell-and-tube storage units and found 25% and 41% improvements in charging and discharging processes, respectively.

Mehta et al. [20] studied various types of shell-and-tube structures and concluded that the rotating structure is thermally more efficient than both eccentric and multitube structures. Selimefendigil and Öztop [21] performed a numerical simulation of a rotating cylinder inside a cavity filled with PCM and showed significant enhancement in heat transfer rates as a result of rotations. The experiments and numerical investigations performed by Fathi and Mussa [22,23] have shown that rotations of tubes have only a moderate effect on liquid fraction and melting behavior. Jaberi Khosroshahi and Hossainpour [24] proved that rotation of the whole system is capable of reducing melting times and improving energy storage efficiency.

Apart from this, recent works have been carried out on the improvement of the thermal performance of latent heat thermal energy storage systems using experimental and theoretical approaches. Aljumaily et al. [26] carried out an experimentally and theoretically based analysis for the enhancement of latent heat thermal energy storage systems and proved that the proper design and conditions can greatly enhance heat storage and recovery performances. In their another study, Aljumaily et al. [27] investigated the effect of the inner tube geometry on the solidification performance of phase change materials and showed that the geometry of the tubes has an essential role in the control of heat transfer and solidification performances of phase change materials. These results further reveal the necessity of optimization of geometrical and operational parameters in latent heat storage applications.

Beside the usual latent heat storage systems, there have been many studies on the improvement of thermal management and energy usage in thermal systems. In previous studies [28–32], it has been shown that proper thermal enhancement techniques and heat transfer mechanisms greatly improve thermal performance. Abeda et al. [33] demonstrated that operational parameters also have an essential role in the determination of the efficiency of thermal systems. In addition, Aljumaily et al. [34] reported that the incorporation of phase change materials into thermal management systems provides effective temperature regulation and enhanced thermal performance. Collectively, these studies highlight the critical role of thermal energy storage and heat-transfer enhancement technologies in achieving sustainable and energy-efficient thermal systems.

Thermal energy storage technologies have also been successfully integrated with solar-energy systems to improve energy utilization and operational stability. Ahmed et al. [27–34] investigated several photovoltaic/Trombe-wall configurations and demonstrated that thermal management and heat-storage techniques can significantly improve both thermal and electrical performance. More recently, Saleh Aljumaily et al. [32] reported substantial enhancement in photovoltaic cooling performance through the integration of paraffin-based phase change materials and trisodium-phosphate solutions under arid climate conditions. These studies highlight the growing importance of thermal storage technologies in renewable-energy applications and support continued research into advanced latent heat storage systems.

Though there is an abundance of experimental studies dealing with shell-and-tube latent heat storage systems, most of the methods used to enhance performance are related to the implementation of fins, eccentric tubes, and multi-tubes. At the same time, the effect of rotation in the same operating conditions has not been studied experimentally extensively enough. Moreover, most of the previous publications concentrate mainly on the charging process (melting), while only a few studies address the effect of rotation on the discharging process (solidification). Besides, there are a few comparisons of stationary and rotating configurations in the same operating conditions.

This paper adds to the existing body of literature in three key ways. First, it compares the stationary and rotating configurations of a shell-and-tube latent heat storage system in the same operating conditions. Second, it uses temperature measurements together with the validated three-dimensional numerical model to reveal the transient behavior of paraffin wax solidification in different axial and circumferential locations.

II. EXPERIMENTAL SETUP AND TEST PROCEDURE

The experimental set-up was developed and constructed in order to study the thermal behavior of the latent heat thermal energy storage system during operation under specified conditions. The test section was comprised of a horizontal carbon steel shell filled with paraffin wax as the PCM inside which an inner concentric tube was placed. The shell had two service ports on the top and bottom for venting and draining purposes, while there were three measurement stations (namely A, B, and C) in the longitudinal direction for measuring the temperature field inside the storage medium. Each of the stations had thermocouple ports installed at the angles of 0°, 45°, and 90°. For providing the necessary heat energy, four electric heaters in the form of annulus with a combined power of 2160 W were fixed on the exterior surface of the shell assembly. Heat losses to the surroundings were reduced by the use of a triple insulation material made up of ceramic fiber, glass wool, and a tin outer cover. The heat transfer fluid (HTF) was circulated within the internal carbon steel pipe in the form of a closed water loop circuit consisting of a galvanized storage tank, a centrifugal pump, and a flow control valve. Temperatures were measured using nine calibrated K-type thermocouples placed within the three measurement sections and were interfaced with a digital temperature data acquisition system. In addition, an electrical control panel was utilized to control the operation of the heater via the thermostat control scheme to provide constant thermal boundary conditions for the tests. In order to study the effect of rotation on the heat transfer process, a worm gearbox drive system was attached to the test equipment to provide the necessary torque and rotation speed in a reliable manner. The major geometrical parameters of the shell, inner tube, heating system, measurement instruments and insulating material are presented in Tables 1 and 2. The scheme of measurement stations, thermocouple placement and measurement instruments is shown in Figs 2 and 3. Prior to every test, preliminary inspections were conducted to check leveling of the system, insulation state, water level, electrical contacts, position of thermocouples and presence of leaks.

The equation representing the instantaneous energy transfer from the phase change material to the heat transfer fluid during the solidification process is expressed as follows [12].

$$q_{dis} = \dot{m}\, C_P\, (T_{f,out} - T_{f,in})$$
(2)

$$Q_{dis} = \sum q_{dis\&ch} \Delta t$$
(3)

In Eqs. (2) and (3), $\dot{m}$and $C_p$represent the mass flow rate and specific heat capacity of the heat transfer fluid (HTF), respectively, while $T_{f,in}$and $T_{f,out}$denote the inlet and outlet temperatures of the circulating water.

In transient state operation, the equation for energy accumulative discharging can be expressed as follows:

$$Q_{H.E,,dis} = M_{H.E}\, C_{p,H.E}(T_{ini} - T_{end})$$
(5)

Where $T_{PCM,i}$and $T_{PCM,f}$represent the initial and final temperatures of the paraffin wax, respectively. The parameters $m_{HX}$and $C_{p,HX}$denote the mass and specific heat capacity of the heat exchanger structure

$$Q_{PCM,dis\,\&} = Q_{\,dis} - Q_{H.E,\ dis}$$
(6)

The theoretical thermal efficiency of the latent heat thermal energy storage (LHTES) unit is defined as:

$$\eta_{THEO} = \frac{Q_{PCM,dis}}{Q_{max,dis}}$$
(7)

The total energy exchanged by the phase change material (PCM) during the solidification process, representing the theoretical maximum energy, can be expressed as follows:

$$Q_{max,dis} = M_{pcm}[C_{P\ pcm}(T_{ini} - T_{liquidus}) + C_{P\ pcm}(L * F)\,(T_{liquidus} - T_{solidus})]$$ (8)

Where $T_s$and $T_l$denote the solidus and liquidus temperatures of the PCM, respectively. Furthermore, $m_{PCM}$and $C_p$represent the PCM mass and specific heat capacity, while Ldenotes the latent heat of fusion and Frepresents the liquid fraction.

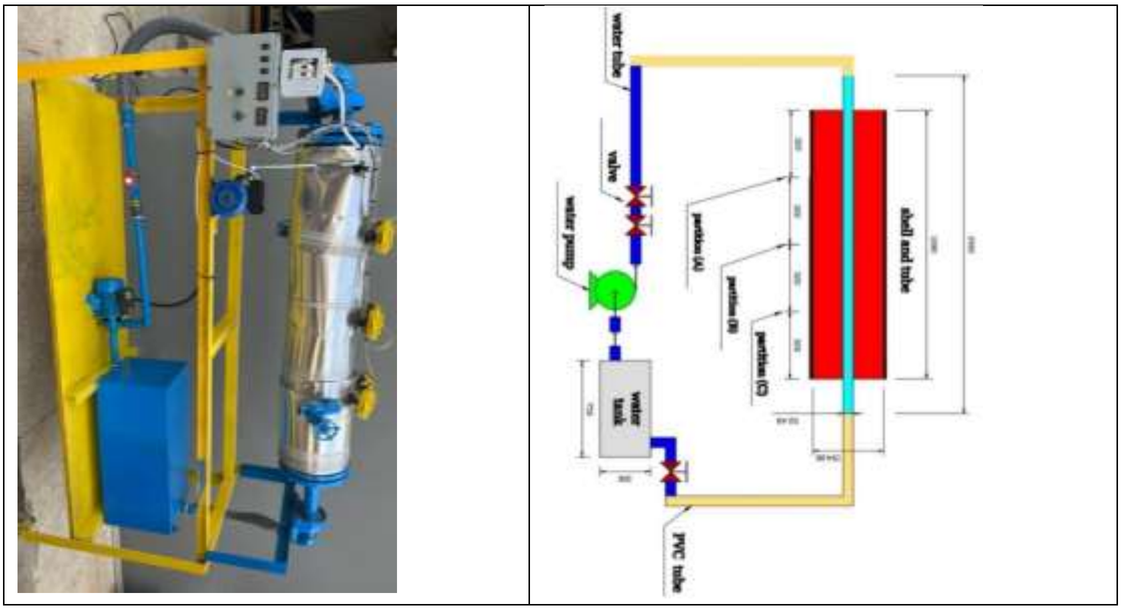

Fig 2: An illustration of the experimental system is provided, with all dimensions given in millimeters.

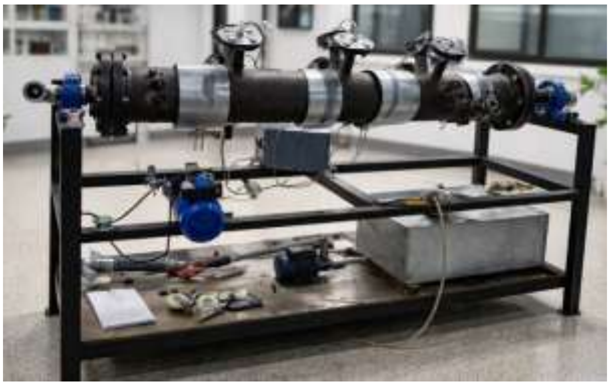

Fig 3: Annular heater connected to the shell.

Table 1. Summary of the Experimental Setup Components and Operating Specifications

Category	Component	Material/Type	Main Dimensions	Thermal/Operating Characteristics
Test Section	Shell	Carbon steel	L=1.28 m, OD=0.1683 m, ID=0.15408 m	Three measuring sections (A–C)
Test Section	Inner tube	Carbon steel	L=2 m, OD=0.0603 m, ID=0.05248 m	HTF flow passage
Heating System	Annular heaters	Electric	Diameter = 0.5 m	Total power = 2160 W
Insulation	Ceramic fiber / Glass wool / Tin sheet	Composite	2.5 mm / 1 mm / 0.5 mm	Reduced heat loss
Hydraulic System	Water tank + pump	Galvanized steel	Capacity = 67.5 L	Pump flow rate = 30 L min^{-1}
Instrumentation	K-type thermocouples	Ni–Cr	9 sensors	±0.75 %, −50–800 °C
Drive System	Worm gearbox	Mechanical transmission	—	Speed reduction and torque increase

Table 2. Thermophysical Properties of Utilized Materials

Property	Paraffin Wax (PCM)	Water	Insulation
Melting point (K)	334	Not specified	Not specified
Solid density (kg/m^3)	894.56	–	–
Liquid density (kg/m^3)	783.42	998.2	–
Specific heat of the liquid (J/kg·K)	2460	4182	–
Specific heat of the solid (J/kg·K)	1659	–	–
Thermal conductivity in solid phase (W/m·K)	0.259	–	0.043
Latent heat of fusion (J/kg)	235,512.5	–	–
Thermal conductivity in liquid phase (W/m·K)	0.158	0.6	–

III. NUMERICAL SIMULATION

The simulation of the PCM solidification process was carried out using ANSYS Fluent 2020 R2 in different configurations for the inner-tube geometry and HTF flow. The enthalpy-porosity model was used for proper modeling of the phase transition and maintaining the energy conservation principle during the charging cycle [5-25].

For simplification of numerical simulation, the following assumptions were made: (i) the HTF comes into the system with the constant temperature of 299 K, and it is considered as an incompressible, laminar, Newtonian fluid; (ii) there is no heat transfer between the outer shell and surroundings, which means that the only heat exchange takes place between the PCM and HTF; (iii) viscous dissipation is ignored; (iv) the PCM (paraffin wax) is homogeneous and isotropic; and (v) the phase change is modeled as a 3D transient problem.

Considering all the above assumptions, the energy conservation equation for temperature and volumetric enthalpy can be represented as follows:

$$\frac{\partial \rho H}{\partial t} + \nabla.(\rho V H) = \nabla.(K \nabla T) + C$$

9

Where $H$is the total volumetric enthalpy, which accounts for both sensible and latent heat contributions. The parameters k, ρ, and Vdenote the thermal conductivity, density, and velocity field of the PCM, respectively.

$$H = H + FL$$

10

$$H = H_{REF} + \int_{TREF}^{T} C_P \, dT$$

11

The liquid fraction Fvaries between 0 and 1 within the mushy zone. Here, $T_{ref}$is the reference temperature, $H_{ref}$is the reference enthalpy, and $C_p$is the specific heat capacity.

$$F = \begin{cases} 0 & T < T_S \\ \frac{T - T_S}{T_L - T_S} & T_S \leq T \leq T_L \\ 1 & T > T_L \end{cases}$$

12

The energy equation, after incorporating Substantial Equations 2 and 4 into Equation 1, is as follows.

$$\frac{\partial \rho H}{\partial t} + \nabla.(\rho V Z) = \nabla.(K \nabla T) - \frac{\partial \rho F L}{\partial t} - \nabla.(\rho V F L) + C$$

13

The momentum equation is expressed as follows:

$$\frac{\partial \rho v}{\partial t} + \nabla.(\rho v v) = -\nabla \mathrm{P} + \nabla.(\mu \, \nabla \, \mathrm{V}) + \rho g + \frac{(1-F)^2}{F^3 + \varepsilon} V A_{mush}$$

14

In this form, ε = 0.001 is a stabilizing parameter that has been used to avoid any mathematical singularity due to division by zero. Here, L refers to the latent heat of fusion, while Amush = 10^5 is a parameter known as the mushy-zone constant that takes care of momentum damping in partially solidified regions in order to prevent any fluid movement in the process of solidification of the PCM.

Moreover, the Boussinesq approximation has been used for buoyancy driven flow due to density variation with temperature. As per this approximation, density is kept constant throughout all equations except the buoyancy term in the momentum equation.

Thereby, natural convection phenomena have been taken care of without increasing computational complexity.

The equation for momentum is given by:

$$\frac{\partial \rho_0 v}{\partial t} + \nabla.(\rho_0 v v) = -\nabla \mathrm{P} + \nabla.(\mu \, \nabla \, \mathrm{v}) + (\rho - \rho_0) g + \frac{(1-F)^2}{F^3 + \varepsilon} v A_{mush} \quad 15$$

$$(\rho - \rho_0) \, g = \beta \, \rho_0 \, (T - T_0)$$

1`6

The continuity equation is expressed as

$$\frac{\partial \rho}{\partial t} + \nabla.(\rho \, v) = 0$$

17

IV. NUMERICAL SETUP

Mesh independency was achieved by performing a sensitivity analysis of the mesh with five different mesh densities. Optimum meshes having 1,452,238, 1,103,634, and 1,099,818 elements were adopted for the circular (Fig. 4). Initially, the temperature of the PCM was kept as 345 K. After conducting a time-step independency analysis, 0.05 s was chosen as the time increment. A limit of 10 iterations was set per each time step for achieving convergence, which led to a total of 365,000 time steps during simulation.

SIMPLE algorithm was utilized for pressure velocity coupling. Momentum and energy equations were discretized using second-order upwind discretization scheme. Pressure interpolation was carried out using second order discretization scheme. Transient terms were treated using a first-order implicit approach. The under-relaxation factors for density, pressure, body forces, liquid fraction, momentum, and energy were set to 1.0, 0.3, 1.0, 0.9, 0.7, and 1.0, respectively. The adopted numerical settings are summarized in Table 3, and the computational meshes are shown in Fig. 5

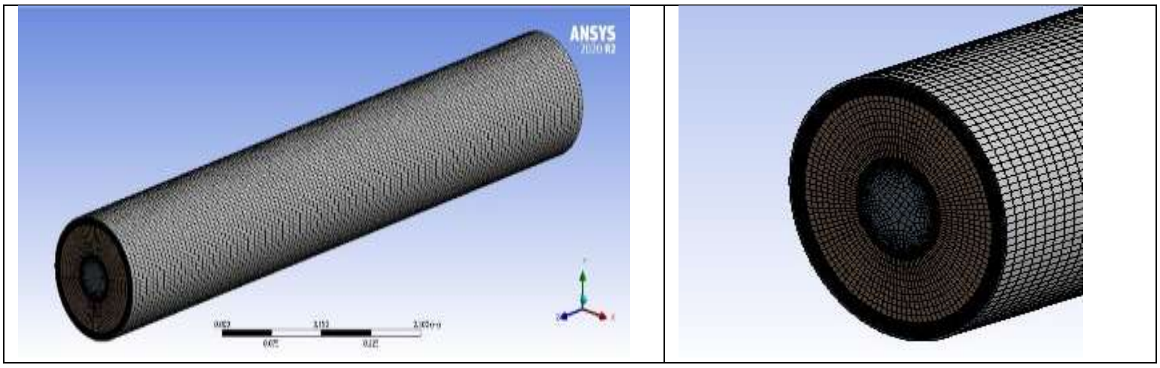

Fig4: Mesh Generation of (A) Circular Tube-Shell, (B) Elliptical Inner Tube with Major-Shell, and (C) Minor Axis Bending-Shell.

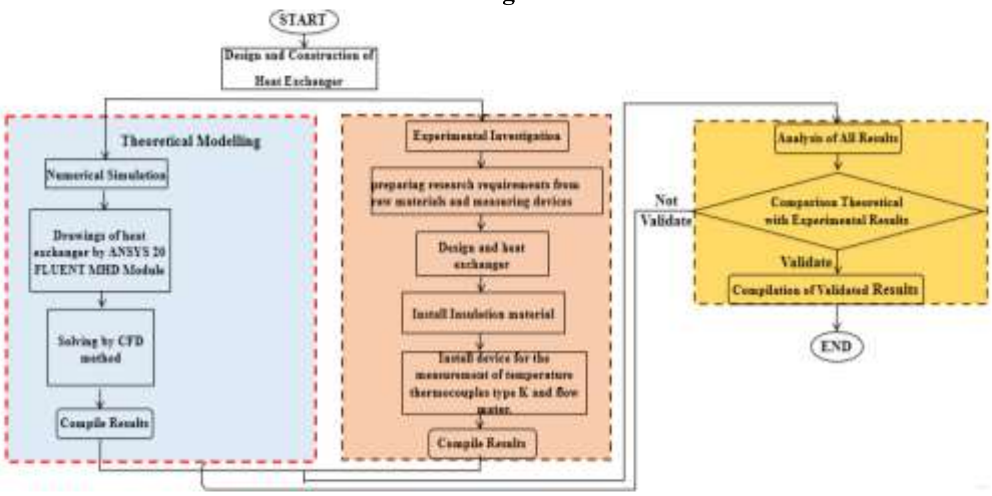

Fig (5): Research methodology.

Table (3): Characteristics of every geometric shape put to the test.

Geometrical Shape	Water Flow Rate (L/min)	Velocity (m/s)	Reynolds Number
Circular tube	2	0.01631	952.36
Total number of tests	3	–	–

V. ANALYSIS OF UNCERTAINTY

An uncertainty analysis was conducted to evaluate the accuracy and reliability of the experimental measurements. Since the calculated parameters depend on multiple measured quantities, the uncertainty associated with each measurement contributes to the overall uncertainty of the final results. Therefore, the total experimental uncertainty was determined using the error propagation method, which combines the uncertainties of all independent variables involved in the calculations [26-27].

For a parameter Texpressed as a function of independent variables $(S_1, S_2, S_3, \dots, S_n)$, the combined uncertainty can be estimated by considering the contribution of each variable to the overall measurement error. This methodology provides a systematic and reliable framework for quantifying experimental uncertainty and assessing the confidence of the reported findings [26-27].

T = T (S1, S2, S3, ……,Sn) (18)

And, the subsequent formula states the relation between the proportions of certain discrepancies in the parameters.

$$\partial N = \frac{\partial T}{\partial S_1}\partial S_1 + \frac{\partial T}{\partial S_2}\partial S_2 + \frac{\partial T}{\partial S_3}\partial S_3 + \dots + \frac{\partial T}{\partial S_n}\partial S_n \quad (19)$$

Also, results (NT) uncertainty is stated by:

$$N_T = \left[\left(\frac{\partial T}{\partial S_1}N_1\right)^2 + \left(\frac{\partial T}{\partial S_2}N_2\right)^2 + \left(\frac{\partial T}{\partial S_3}N_3\right)^2 + \dots + \left(\frac{\partial T}{\partial S_n}N_n\right)^2\right]^{\frac{1}{2}} \quad (20)$$

Dividing equation (12) by equation (10) gives

$$\frac{N_T}{T} = \left[\left(\frac{\partial T}{\partial S_1}\frac{N_1}{T}\right)^2 + \left(\frac{\partial T}{\partial S_2}\frac{N_2}{T}\right)^2 + \left(\frac{\partial T}{\partial S_3}\frac{N_3}{T}\right)^2 + \dots + \left(\frac{\partial T}{\partial S_n}\frac{N_S}{T}\right)^2\right]^{\frac{1}{2}} \quad (21)$$

And, the error created through the use of the measuring instruments for the temperature and the rate of flow are (+/-0.75%) and (+/-4%) for the temperature and the rate of mass flow respectively. Furthermore, the error calculated for the rate of heat transfer equation is dependent on many factors.

$Q^{\cdot} = F(\Delta T, \dot{m})$
(22)
$\frac{\partial Q}{\partial \dot{m}} = C_P \Delta\, T^{\cdot}$
(23)
$\frac{\partial Q}{\partial \Delta T} = C_P \dot{m}$
(24)
And, heat transfer (NQ) uncertainty is stated as:
$\frac{N_Q}{Q} = \left[\left(\frac{\partial Q}{\partial \dot{m}}\frac{N_{\dot{m}}}{Q}\right)^2 + \left(\frac{\partial Q}{\partial\, \Delta T}\frac{N_{\Delta T}}{Q}\right)^2\right]^{\frac{1}{2}}$
(25)
Where:
$N_{\dot{m}} = error_{\dot{m}}\dot{m}$
(26)
$N_{\Delta T} = error_{\Delta T}\Delta T^{\cdot}$
(27)
Substituting the whole terms values into equation 25 gives :
$\frac{N_Q}{Q} = 6\%$

VI. RESULTS AND DISCUSSION

Solidification tests started when the paraffin wax was completely melted and the temperature of the PCM was measured to be around 345 K, and the circulation of cold water through the inner tube helped in extracting heat from the energy storage material. Measurements of temperature and liquid fraction were taken every two minutes at three different axial-radial points (A, B, and C) so as to make an effective evaluation of the transient thermal behavior under stationary and rotating modes. As seen in Fig 6, the solidification process started from the inner tube and progressed to the outer shell; hence, it is evident that heat extraction from the HTF side played an important role in the early stage of discharge.

Fig 6 shows the temporal development of the liquid fraction throughout the solidification process of the PCM in both stationary and rotating systems. In all cases, the solidification process took place through the radial motion of the solidification interface from the inside of the inner tube to the shell wall as a result of continuous cooling of the system using the heat transfer fluid. The solidification of the lower part of the storage device (at 0°) took place before the inclined (at 45°) and the upper parts (at 90°), demonstrating the effect of buoyancy on thermal stratification in the molten PCM.

The temperature fraction of the PCM in Fig 7 indeed shows a constant decrease in all cases considered, and the thermal field shows better homogeneity with the progress of the solidification process. The agreement in the temperature distributions measured numerically and experimentally proves that the thermal model is correct, since it reflects the heat transfer processes to an acceptable level of accuracy using the chosen boundary conditions and material parameters. It should be noted that the rate of temperature decrease was faster in the rotating case.

The results clearly reveal that the rotational motion improves the solidification efficiency of the shell and tube latent heat storage system through the mitigation of thermal stratification, acceleration of liquid fraction decrease, and improving temperature uniformity inside the PCM domain. The degree of enhancement is different depending on the location and operation condition. Therefore, it can be concluded that the rotation effect must be considered as an optimizing factor rather than a universal factor. The simulation results showed a good agreement with the experiments and could be used for predictions.

The variations in temperature experimental at the three measuring locations (A, B, and C) are presented in Fig 8. Location A had the highest reduction in temperature, indicating higher interaction between the HTF and the PCM at the upstream end of the heat exchanger. Location B and C had lower reductions in temperature, showing increasing thermal resistance due to thicker solid layer and greater heat transfer pathway length. This variation along the axial direction is common in shell and tube latent heat storage devices and indicates that the discharging process operates under a combination of conduction and convection.

From the experimental and numerical energy-based results shown in Fig 9, it can be observed that there is an increase in the amount of heat absorbed by the HTF, the total energy transfer from the PCM, and thermal efficiency with time. In addition, the rotating setup always performed better than the static setup. At a flow rate of 2 L/min, the static circular setup attained a heat gain of 1117.8 kJ after 310 minutes, whereas the total energy transferred from the PCM to the HTF was 1045.2 kJ at 240.5 minutes for the same operating condition and the same fraction of the liquid. It must be emphasized that the current study was carried out at a fixed flow rate of heat transfer fluid and using one particular phase change material under the existing geometry. It is essential to stress that the current results may have significant practical significance regarding latent heat thermal energy storage systems. In view of the fact that there is an increase in temperature uniformity and solidification rate due to rotation, it could be concluded that the use of rotation could be considered as an approach in passive/semi-passive control of thermal storage systems that require rapid energy release.

VII. VALIDATION CASE STUDY

The results obtained from the present study in relation to solidification of PCM in the circular tube have been compared with those obtained from the previous literature work [25-36]. In the work done by Seddegh et al. [36], the numerical study of energy storage has been done for a horizontal shell and circular inner tube system with Paraffin wax (RT 50) that melts in the temperature range of 318-324

K. In the experiment, the flow rate of water was 2.5 l/min. The shell has been made of iron with interior diameter 85 mm and thickness of 2.5 mm while the inner tube was made of copper and is located at the center of the shell with diameter 22 mm. In the current work, the heat exchanger made of Paraffin wax with melting temperature 345 K and aluminum shell having inner diameter 160 mm and thickness 1.5 mm has been analyzed. The inner tube, composed of copper, was positioned at the center with a diameter of 54 mm. Both investigations utilized water as the heat transfer fluid (HTF) that cycled through the inner tube. The findings demonstrated a strong alignment between the current and prior results, as depicted in **Fig 10 and Table 4**. Furthermore, the results demonstrated a strong correlation between the experimental investigations of thermal efficiency and numerical simulation, as depicted in **Fig 6.**

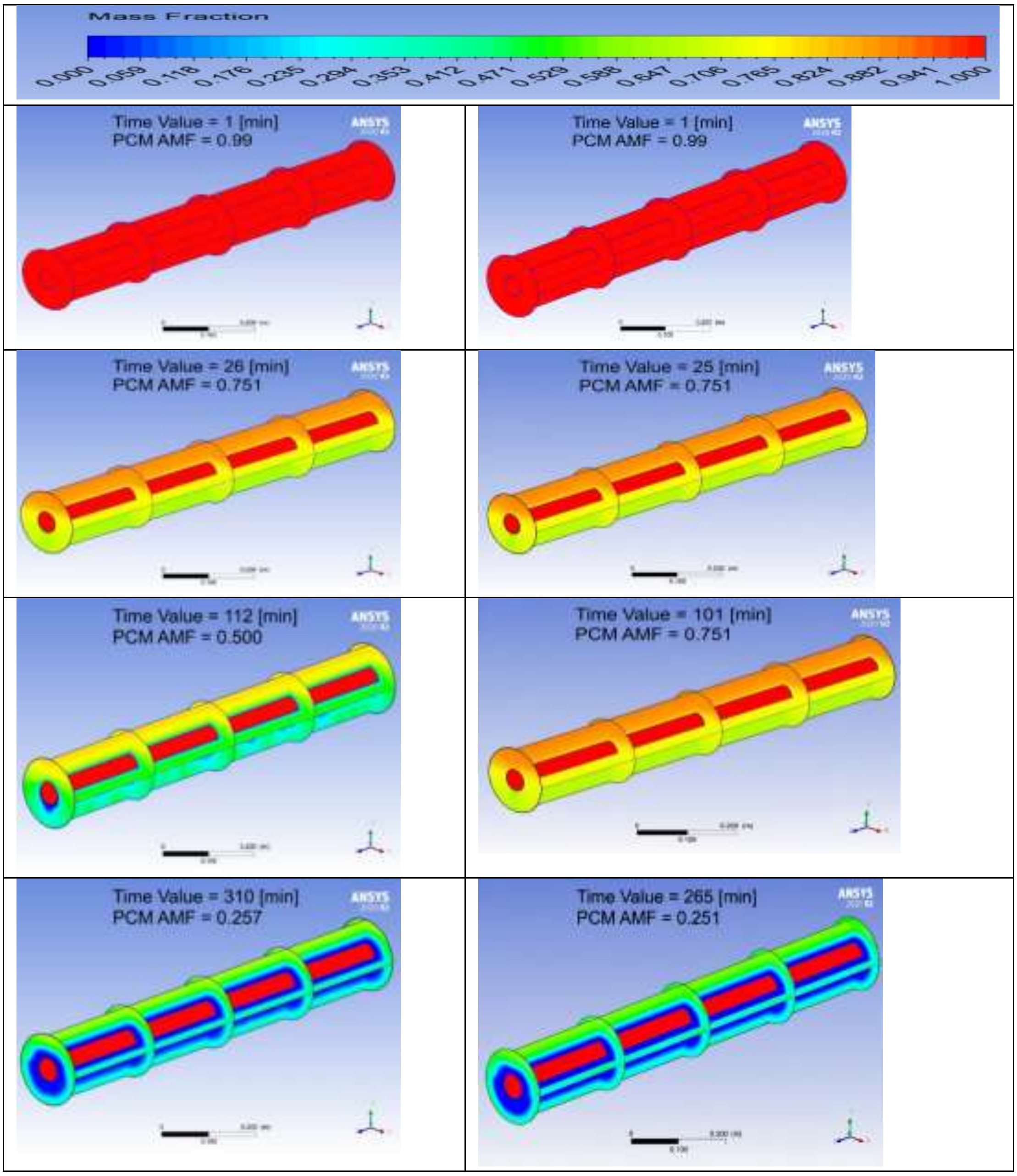

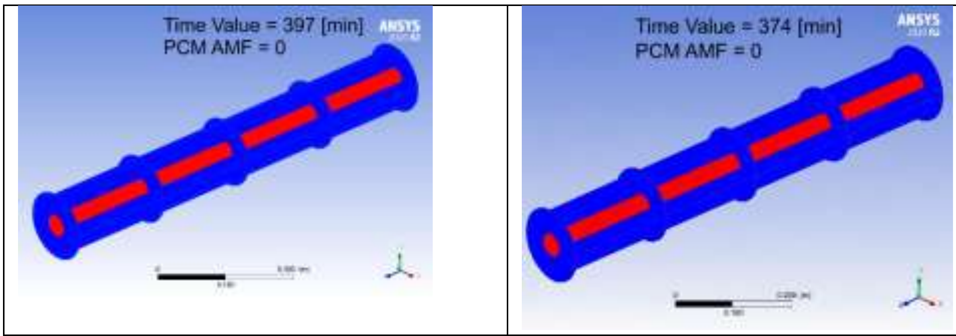

Static	With Rotation

Fig 6: Temporal evolution of liquid fraction during PCM solidification for stationary and rotating configurations at 2 L/min.

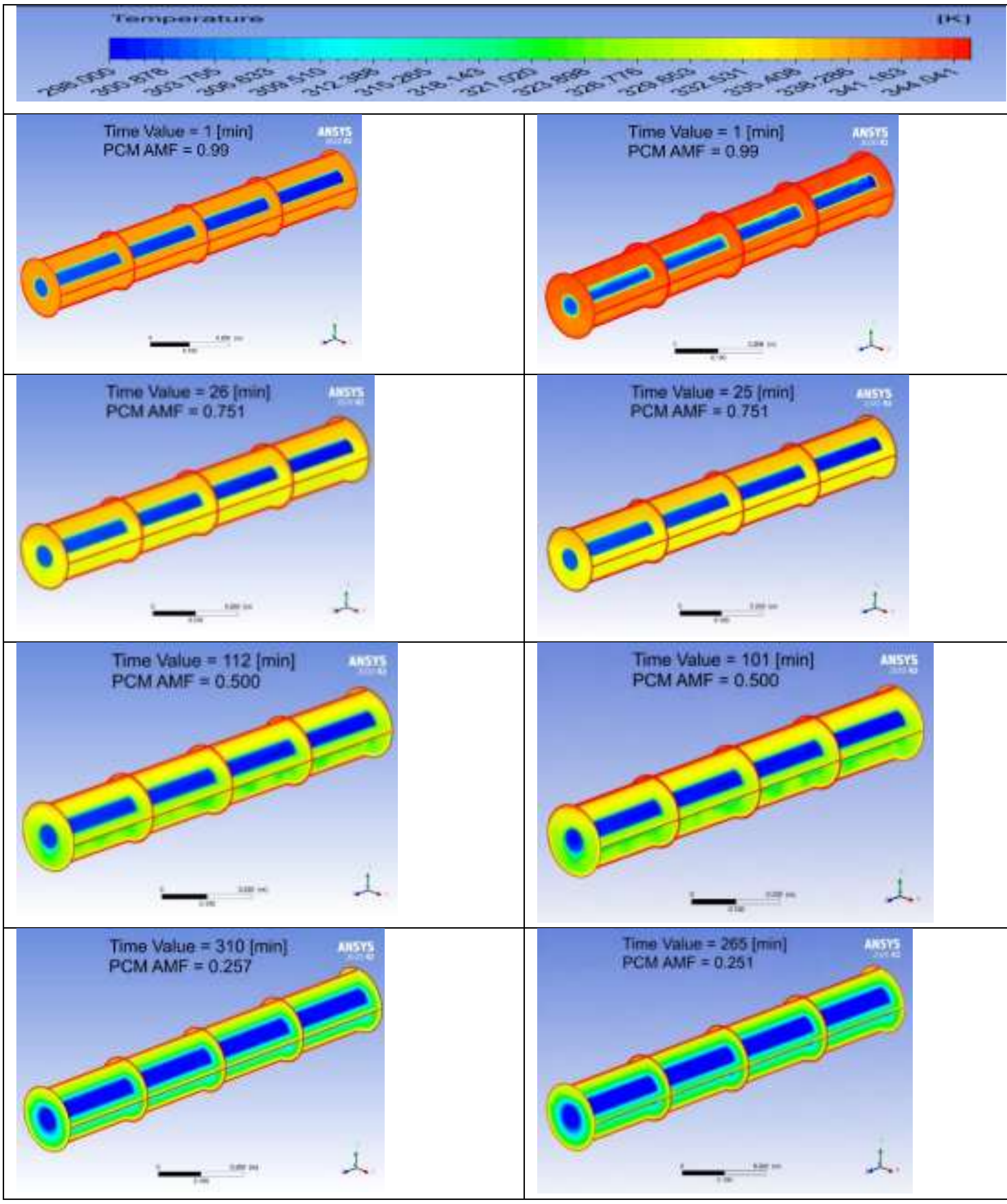

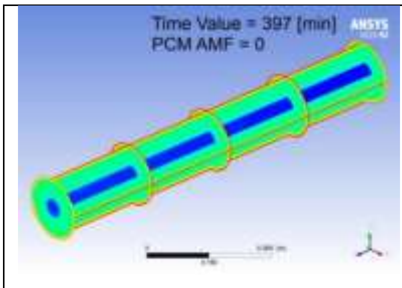	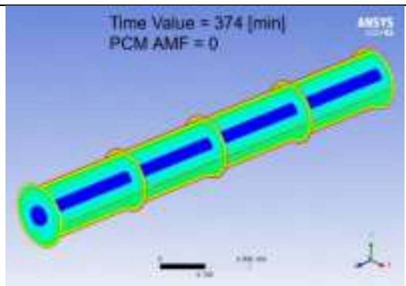
Static	**With Rotation**

Fig. 7 Theoretical and experimental temperature contours during PCM solidification for stationary and rotating configurations at 2 L/min.

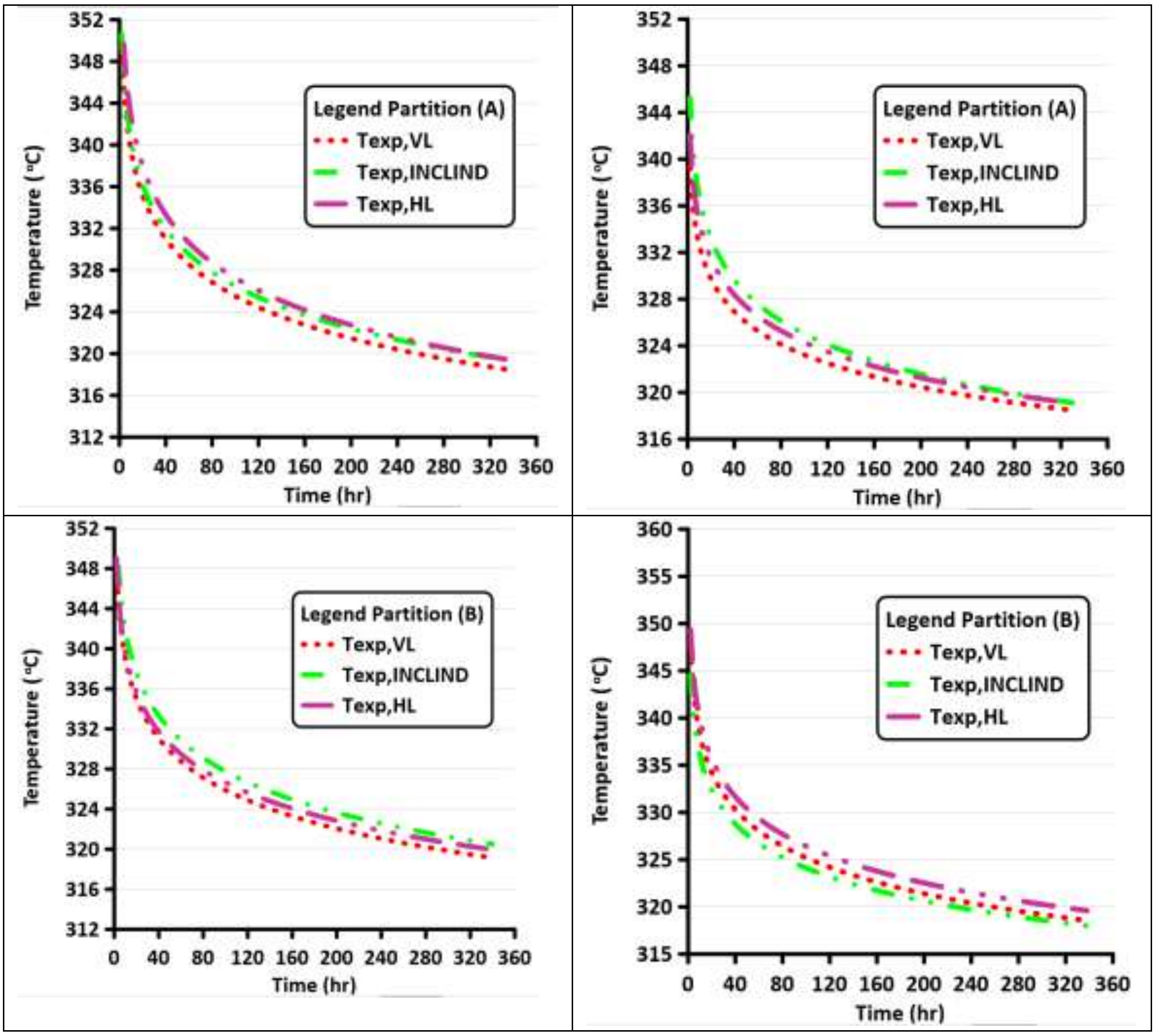

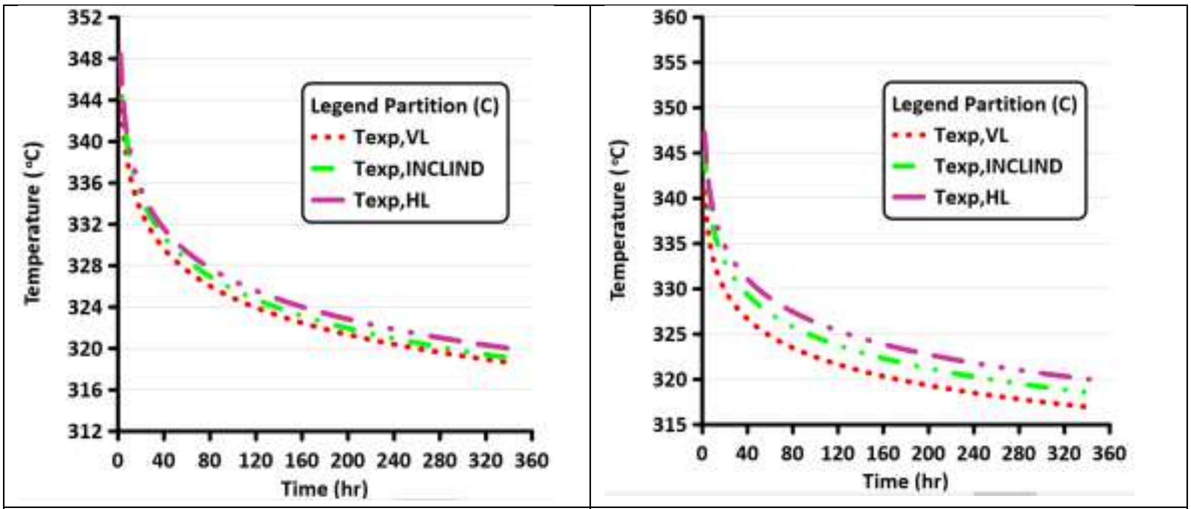

Static	With Rotation

Fig 8: Experimental temperature variation with time at three partitions of the LHES unit (A, B, and C) during PCM solidification.

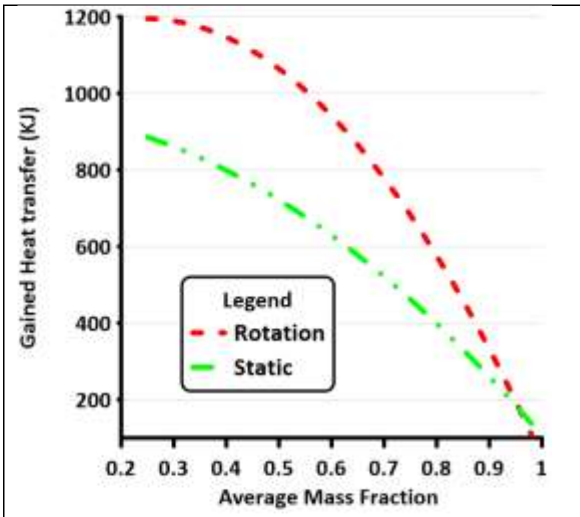

(A) Gained Heat transfer (KJ)

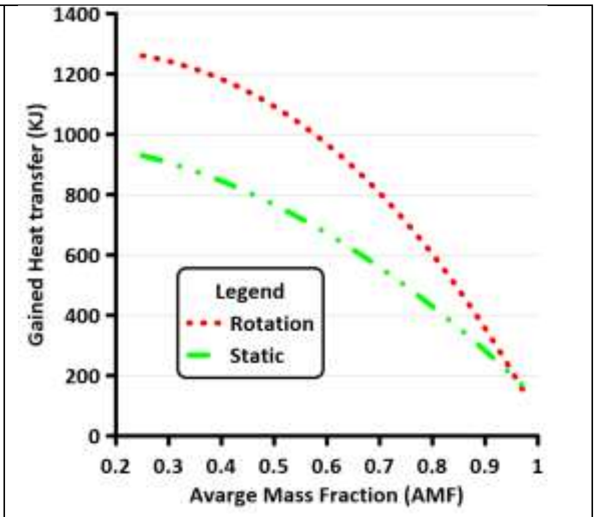

(A) Gained Heat transfer (KJ)

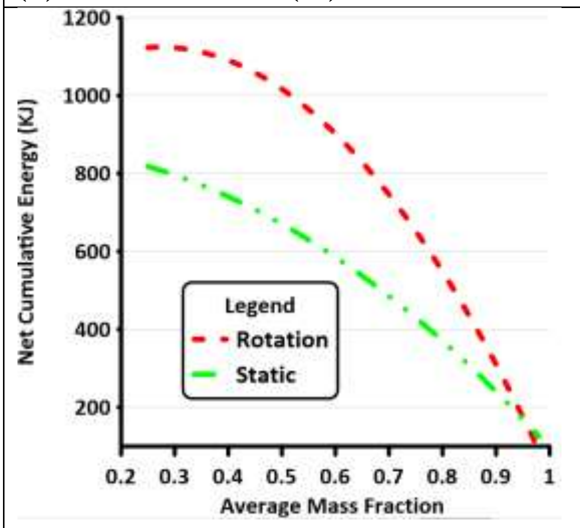

(B) Net Cumulative Energy (KJ)

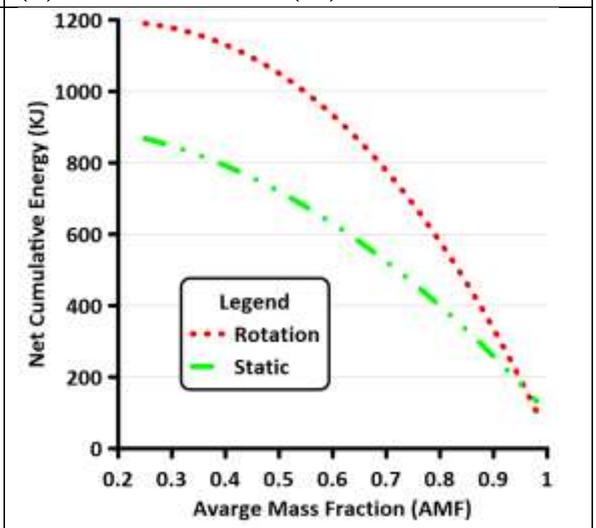

(B) Net Cumulative Energy (KJ)

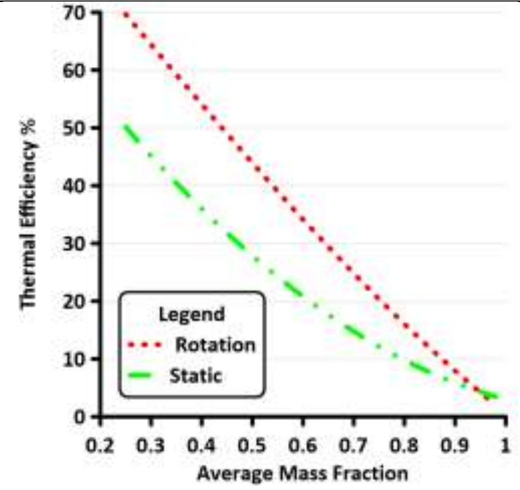	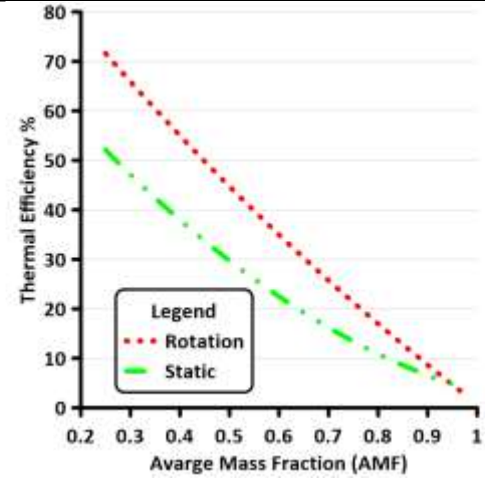
(C) Thermal Efficiency %	(C) Thermal Efficiency %
Theortical	Expermental

Fig. 9: Comparison of heat gain, net cumulative energy, and thermal efficiency for theoretical and experimental cases

Table 4. Comparison results for validation case study

Mass fraction	Time (min) for Present results	Time (min) for Results of [36]
0.99	1	1
0.5	112	120
0	397	450

A: Present results

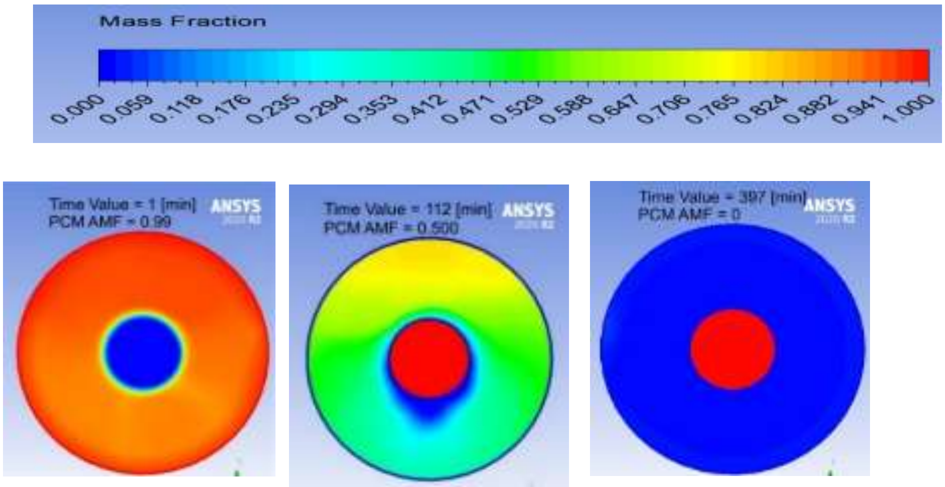

B: Results of [51]

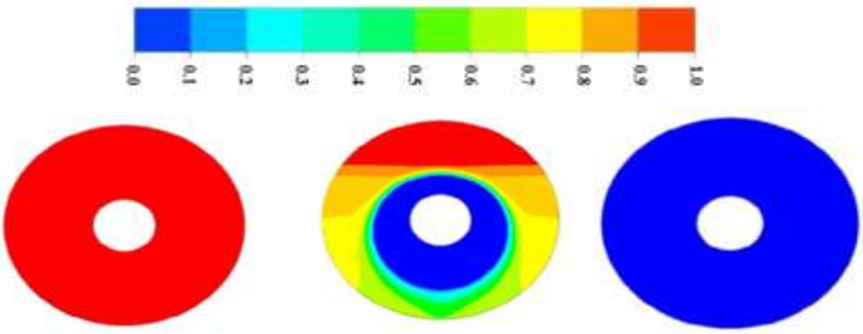

0 (min) 120 (min) 450 (min)

Fig 10. The validation of the numerical investigation for the contours of the fraction of liquid through the procedure of discharging in a horizontal regime.

VIII. CONCLUSIONS

This study presented a combined experimental and numerical investigation of the solidification behavior of paraffin wax in a horizontal shell-and-tube latent heat thermal energy storage unit operating under stationary and rotational conditions. thermal energy storage unit for latent heat using stationary and rotational modes. The effect of rotation on liquid-fraction changes, temperature profile, heat transfer behavior, and energy recovery efficiency was investigated thoroughly.

From the above analyses, the following observations have been made:

1. The solidification process followed the principle of both conduction and convection mechanisms. In the early stage of discharge, natural convection played an important role in heat transfer within the molten PCM, while conduction mechanism became the dominant mode as the solidification progressed and the thickness of solidified layer increased around the inner pipe.

2. The thermal field showed obvious spatial non-uniformity, with the bottom part (0° position) undergoing solidification process faster than the inclined (45°) and upper (90°) sections. This was because of the phenomenon of thermal stratification caused by buoyancy within the PCM region.

3.The rotation motion greatly improved the thermal performance of the energy storage unit. Compared with stationary setup, the rotating model had a faster decrease in liquid-fraction, shorter solidification time, better temperature uniformity, and lower thermal resistance within the PCM region.

4. The rotating design exhibited more favorable characteristics for energy regeneration during the discharge period. Under the conditions explored in the analysis, the heat gain and total energy discharged were equal to 1117.8 kJ and 1045.2 kJ, respectively. Hence, it can be stated that the use of rotational movement improves the performance of the system when recovering energy from the PCM.

5. The proposed numerical model was shown to correctly reproduce the experimental results and was found to agree with previously published benchmark values. This confirms the ability of the enthalpy–porosity method for predicting solidification in shell-and-tube latent heat storage units.

Even though this work clearly demonstrates the effect of rotational movement, there were several limitations in this analysis, as only one flow rate and one type of PCM were used, along with limited geometrical variations. Thus, it is necessary to consider the effects of rotational speed, flow rate, PCM type, tube geometry, and insulation on the performance of latent heat thermal energy storage systems.

REFERENCES

1. Fath HES. Thermal performance of a simple design shell-and-tube latent heat storage unit. Energy Conversion and Management. 1991;31(2):149–155.
2. Lacroix M. Numerical simulation of a shell-and-tube latent heat thermal energy storage unit. Solar Energy. 1993;50(4):357–367.
3. Lacroix M. Study of the heat transfer behavior of a latent heat thermal energy storage unit with fins. International Journal of Heat and Mass Transfer. 1993;36(8):2083–2092.
4. Hosseini MJ, Rahimi M, Bahrampoury R. Experimental and computational evaluation of a shell-and-tube heat exchanger as a PCM thermal storage system. International Communications in Heat and Mass Transfer. 2014;50:128–136.
5. Avci M, Yazici MY. Experimental study of thermal energy storage characteristics of a paraffin in a horizontal tube-in-shell storage unit. Energy Conversion and Management. 2013;73:271–277.
6. Kibria MA, Anisur MR, Mahfuz MH, Saidur R, Metselaar IHSC. A review on thermophysical properties of phase change materials. Renewable and Sustainable Energy Reviews. 2014;39:725–749.
7. Sasaguchi K, Viskanta R, Akiyama M. Heat transfer enhancement in latent heat thermal energy storage systems. Journal of Solar Energy Engineering. 1986;108(3):181–186.
8. Dutta R, Atta A, Dutta TK. Experimental and numerical study of heat transfer in horizontal concentric annulus containing phase change material. Canadian Journal of Chemical Engineering. 2008;86(4):700–710.
9. Darzi AAR, Farhadi M, Sedighi K. Numerical study of melting inside concentric and eccentric horizontal annulus. Applied Mathematical Modelling. 2012;36(9):4080–4086.
10. Agyenim F, Eames P, Smyth M. A comparison of heat transfer enhancement in a medium temperature thermal energy storage heat exchanger using fins. Solar Energy. 2009;83(9):1509–1520.
11. Agyenim F, Eames P, Smyth M. Heat transfer enhancement in medium temperature thermal energy storage system using a multitube heat transfer array. Renewable Energy. 2010;35(1):198–207.
12. Esapour M, Hosseini MJ, Ranjbar AA, Pahamli Y, Bahrampoury R. Phase change in multi-tube heat exchangers. Renewable Energy. 2016;85:1017–1025.
13. Al-Abidi AA, Mat S, Sopian K, Sulaiman MY, Mohammad AT. Internal and external fin heat transfer enhancement technique for latent heat thermal energy storage in triplex tube heat exchangers. Applied Thermal Engineering. 2013;53(1):147–156.
14. Zhao L, Xing Y, Liu X, Rui Z. Heat transfer enhancement in triplex-tube latent thermal energy storage system with selected arrangements of fins.

IOP Conference Series: Earth and Environmental Science. 2018;108:042081.

15. Gong ZX, Mujumdar AS. Thermodynamic optimization of shell-and-tube latent heat storage systems. Heat Recovery Systems and CHP. 1997;17(3):253–264.
16. Tao YB, He YL, Qu ZG, Qiu Y. Numerical study on performance enhancement of phase change thermal storage device with finned tube. Applied Energy. 2012;90(1):83–90.
17. Elbahjaoui R, El Qarnia H. Numerical study of a shell-and-tube latent thermal energy storage unit heated by laminar pulsed fluid flow. Heat Transfer Engineering. 2017;38(17–18):1466–1480.
18. Herrick CS, Zarnoch KP. Heat storage capability of a rolling cylinder using Glauber's salt. International Journal of Ambient Energy. 1980;1(1):47–55.
19. Kurnia JC, Sasmito AP. Numerical investigation of rotating latent heat thermal energy storage systems. Applied Thermal Engineering. 2018;134:221–231.
20. Mehta B, Patel R, Shah N. Numerical comparison of rotating, eccentric and multitube latent heat storage systems. Journal of Energy Storage. 2019;26:100996.
21. Selimefendigil F, Öztop HF. Rotational effects on melting enhancement in PCM-filled enclosures. International Communications in Heat and Mass Transfer. 2020;116:104697.
22. Fathi MI, Mussa MA. Experimental investigation of tube rotation effect on shell-and-tube latent heat energy storage systems. Journal of Energy Storage. 2021;39:102626.
23. Fathi MI, Mussa MA. Numerical investigation of tube rotation influence on PCM melting process in latent heat energy storage systems. Journal of Engineering. 2021;27(11):1–16.
24. Jaberi Khosroshahi S, Hossainpour S. Numerical study of continuous and stepwise rotation effects on latent heat thermal energy storage systems. Journal of Energy Storage. 2021; 35:102300.
25. Elmeriah A, Nehari D, Aichouni M. Thermo-convective study of a shell-and-tube thermal energy storage unit. Periodica Polytechnica Mechanical Engineering. 2018;62(2):101–109.
26. Aljumaily, A. M. S., Al-Jubouri, A. A. H., & Al-Jubouri, N. F (2023). Improving the Thermal Storage System (LHTES): A theoretical and experimental study. https://doi.org/10.2139/ssrn.4427085
27. Aljumaily, A. M. S., Mohammed, A. A., & Aljabair, S. Effect of Inner Tube Shapes in a Heat Exchanger on a Solidification of Phase Change Material. Available at SSRN 4427085 https://doi.org/10.2139/ssrn.4427962
28. Ahmed, O. K., Hamada, K. I., & Salih, A. M. (2019). Enhancement of the performance of Photovoltaic/Trombe wall system using the porous medium: Experimental and theoretical study. Energy, 171(Mar), 14-26. https://doi.org/10.1016/j.energy.2019.01.001
29. Ahmed, O. K., Hamada, K. I., & Salih, A. M. (2022). Performance analysis of PV/Trombe with water and air heating system: an experimental and theoretical study. Energy Sources, Part A: Recovery, Utilization, and Environmental Effects, 44(1), 2535-2555. https://doi.org/10.1080/15567036.2019.1650139
30. Ahmed, O. K., Hamada, K. I., Salih, A. M., & Daoud, R. W. (2020). A state of the art review of PV-Trombe wall system: Design and applications. Environmental Progress & Sustainable Energy, 39(3), e13370. https://doi.org/10.1002/ep.13370
31. Ahmed, O. K., Hamada, K., & Salih, A. (2019, June). Thermal and Electrical Performance Analysis of PV/Trombe Wall System. In 2019 International Engineering Conference (IEC) (pp. 68-73). IEEE. https://doi.org/10.1109/IEC47844.2019.8950524
32. Ahmed, O., Hamada, K., Salih, A., & Daoud, R. (2020, September). Performance Improvement of Bi-Fluid Photovoltaic/Trombe Wall Using Glass Cover and Porous Medium. In Proceedings of the 1st International Multi-Disciplinary Conference Theme: Sustainable Development and Smart Planning, IMDC-SDSP 2020, Cyperspace, 28-30 June 2020. DOI 10.4108/eai.28-6-2020.2297888
33. Abeda, A., Mohammed, A., Ali, H. A., Abidb, M., & Jasim, (2023). A numerical analysis of the operational factors influencing the effectiveness of a building air conditioning systems employing geothermal energy.
34. Saleh Aljumaily, A. M., Ali, A. Y., & Oglah, M. H. (2026). Experimental and Theoretical Study of PV Cooling Using Paraffin PCM and Trisodium-Phosphate (TSP) Solution in Arid Climates. *Progress in Photovoltaics: Research and Applications*. https://doi.org/10.1002/pip.70082
35. Seddegh, S., Joybari, M. M., Wang, X., & Haghighat, F. (2017). Experimental and numerical characterization of natural convection in a vertical shell-andtube latent thermal energy storage system. Sustainable cities and society, 35, 13-24.
36. Seddegh, S., Wang, X., & Henderson, A. D. (2015). Numerical investigation of heat transfer mechanism in a vertical shell and tube latent heat energy storage system. Applied thermal engineering, 87, 698-706.